

Reflectance tomography of two-layered turbid media with diffuse photon-density waves

Thorsten Spott^a, Lars O. Svaasand^a, Joshua B. Fishkin^b, Tuan Pham^b and Bruce J. Tromberg^b

^aDept. of Physical Electronics
Norwegian University of Science and Technology (NTNU)
N-7034 Trondheim
Norway

^bBeckman Laser Institute and Medical Clinic
University of California
1002 Health Sciences Rd. East
Irvine, CA 92612
USA

ABSTRACT

An approach to the examination of the structure of layered tissue can be found in the measurement of the diffuse reflectance of plane diffuse photon-density waves in the near-infrared range. Here, phase resolved reflectance measurements from phantom tissue, at modulation frequencies of up to 2 GHz, are presented and compared to calculations provided by a theoretical model. The examination of the phase shift reveals that the reflectance properties are characterized by photon-density wave interference phenomena. The proposed technique allows the investigation of the structure of tissue down to more than one penetration depth. A medical application may be found in improved examination techniques for deep burns, as the method allows the investigation of the tissue structure without physical contact to the surface.

Keywords: Diffuse photon-density waves, reflectance tomography, layered media, phase shift

1. INTRODUCTION

Optical reflectance tomography offers the attractive possibility of non-invasive examination of biological tissue. Light enters the tissue and, after having traveled over a certain path length, it partly reappears at the surface, ready to be analyzed. By comparing the incident to the reappearing light, valuable information can be gained about the optical properties of the tissue and, by further interpretation, about its medical condition. As biological tissues tend to be highly scattering, optical techniques based on the coherence of light can only be used for examinations at depths of a fraction of the penetration depth.^{1,2} In order to obtain data from greater depths, multiple scattering has to be dealt with. In the limit, diffusion models for light propagation assume that coherence is altogether lost. Light that has randomly traveled in the tissue and reappears at the surface, i.e. diffusely reflected light, can carry information about more than one penetration depth into the tissue. This implies that, depending on the tissue under investigation, it potentially has traveled through several layers of different optical properties and eventually carries a mixture of influences from all of them. This compound effect of layers with different optical properties on light propagation has been addressed in several studies.³⁻¹¹ In some medical settings, the evolving phenomena are considered disturbing, in other cases they are explicitly wanted for analyses of the structure of the tissue. The former case is often met when the tissue under examination is buried in some other type of tissue. The photons bearing information on the portion of the tissue that is of interest lose part of this information during propagation through circumjacent tissue

Other author information:

T.S.: Email: thorsten@fysel.ntnu.no; Phone: ++47/73 59 44 16; Fax: ++47/73 59 14 41
L.O.S.: Email: lars.svaasand@fysel.ntnu.no; Phone: ++47/73 59 44 21; Fax: ++47/73 59 14 41
J.B.F.: Email: jfishkin@bli.uci.edu; Phone: ++1/(949) 824-4713; Fax: ++1/(949) 824-8413
T.P.: Email: tpham@bli.uci.edu; Phone: ++1/(949) 824-4713; Fax: ++1/(949) 824-8413
B.J.T.: Email: tromberg@bli.uci.edu; Phone: ++1/(949) 824-8705; Fax: ++1/(949) 824-8413

and by mixing with light that has never reached the location under investigation. As the structural properties of macroscopically inhomogeneous tissue can be complicated or even unknown, a homogeneous tissue is often assumed a priori in order to make mathematical modeling feasible.^{12,13} However, a better understanding of how the measurement is affected by different types of tissue could greatly improve such measurements. This problem was recently studied by Farrell and coworkers.⁹ An investigation by Kienle et al.¹⁰ proposed a method for extracting the optical properties of a single layer from the diffuse reflectance from a two-layered structure.

The latter case, the possibility of using the diffusely reflected light for extraction of structural information, was addressed by Cui and Ostlander,⁸ who realized that photons re-emerging rather distantly from their point of insertion are more likely to have traveled deeper into the tissue than those leaving the tissue close to the irradiated area. A promising technique for structural investigations is based on *diffuse photon-density waves* (DPDW), which are excited by sinusoidally intensity modulating the incident light.¹⁴⁻¹⁷ The investigations by Farrell et. al and Kienle et al. mentioned above also follow this approach. The penetration depth, which is complex in the case of intensity modulated light, depends both on the optical properties of the tissue and the modulation frequency. The dispersion properties of diffuse photon-density waves show that the phase velocity increases with increasing absorption, and with decreasing scattering.¹⁵ This effect depends, moreover, on the modulation frequency. Thus, the phase is delayed differently in tissues of different optical properties, and it must be expected that the interference of waves from adjacent layers can be observed in a phase shift of the diffusely reflected light, relative to the incident light. A first account of this phenomenon, observed in partly coagulated tissue, was recently presented by Svaasand et al.¹¹

This study is aimed at the investigation of the phase properties of the reflection coefficient of two-layered intralipid phantoms, both theoretically and experimentally, when irradiated by an intensity-modulated plane wave.

2. THEORETICAL BACKGROUND

2.1. Diffusion approximation to the Boltzmann transport equation¹⁸⁻²⁰

It has been found that light propagation in biological tissue can be adequately described by a corpuscular model which is governed by the Boltzmann transport equation:

$$\frac{1}{c} \frac{\partial L(\mathbf{r}, \mathbf{s}, t)}{\partial t} + \nabla \cdot L(\mathbf{r}, \mathbf{s}, t) \mathbf{s} = -(\mu_a + \mu_s) L(\mathbf{r}, \mathbf{s}, t) + \mu_s \iint_{4\pi} L(\mathbf{r}, \mathbf{s}, t) f(\mathbf{s}, \mathbf{s}') d\Omega' + Q(\mathbf{r}, \mathbf{s}, t) \quad (1)$$

| | | |
|--------|--------------------------------|---|
| where: | $L(\mathbf{r}, \mathbf{s}, t)$ | radiance, $[L] = W/(m^2 \cdot sr)$ |
| | $f(\mathbf{s}, \mathbf{s}')$ | anisotropy factor, $\iint_{4\pi} f(\mathbf{s}, \mathbf{s}') d\Omega' = 1$ |
| | \mathbf{s} | directional unit vector, $[\mathbf{s}] = 1$ |
| | μ_a | absorption coefficient, $[\mu_a] = m^{-1}$ |
| | μ_s | scattering coefficient, $[\mu_s] = m^{-1}$ |
| | $c = c_0/n_{tissue}$ | speed of light, $[c] = m/s$ |
| | c_0 | vacuum speed of light, $[c_0] = m/s$ |
| | n_{tissue} | index of refraction of tissue, $[n] = 1$ |

Unless the blood concentration in the tissue is very high, scattering will dominate absorption (i.e. $\mu_s \gg \mu_a$). Then, the radiance can be approximated by the sum of an isotropic fluence rate φ and a directional flux \mathbf{j} :

$$L(\mathbf{r}, \mathbf{s}, t) \approx \frac{1}{4\pi} \varphi(\mathbf{r}, t) + \frac{3}{4\pi} \mathbf{j}(\mathbf{r}, t) \cdot \mathbf{s} \quad (2)$$

| | | |
|--------|-----------------------------|--|
| where: | $\varphi(\mathbf{r}, t)$ | fluence rate, $[\varphi] = W/m^2$ |
| | $\mathbf{j}(\mathbf{r}, t)$ | diffuse photon flux vector, $[\mathbf{j}] = W/m^2$ |

In a plane symmetry, the vector \mathbf{r} can be replaced by the depth into the tissue z . The flux vector \mathbf{j} can then be expressed by its scalar value, j . In the model described here, the source is assumed to be isotropic. Substituting (2) in (1) and integrating over 4π solid angle yields two decoupled equations, namely the *diffusion equation*:

$$\frac{1}{c} \frac{\partial}{\partial t} \varphi(z, t) + \mu_a \varphi(z, t) + \frac{\partial}{\partial z} j(z, t) = q_0(z, t) \quad (3)$$

and:

$$\frac{1}{c} \frac{\partial}{\partial t} j(z, t) + \mu_{tr} j(z, t) + \frac{1}{3} \frac{\partial}{\partial z} \varphi(z, t) = 0 \quad (4)$$

where:

| | |
|---|---|
| $\mu_{tr} = \mu'_s + \mu_a$ | transport coefficient, $[\mu_{tr}] = m^{-1}$ |
| $\mu'_s = \mu_s(1 - g)$ | reduced scattering coefficient, $[\mu'_s] = m^{-1}$ |
| $g = \iint_{4\pi} f(\mathbf{s}, \mathbf{s}') \mathbf{s} \cdot \mathbf{s}' d\Omega'$ | average cosine of scattering angle, $[g] = 1$ |
| $q_0(z, t) = 4\pi Q(z, t)$ | isotropic source intensity, $[q_0] = W/m^3$ |

For time-harmonic sources, the proportionality $q_0 \sim e^{i\omega t}$ is valid. Eqs. (3) and (4) can then be combined to a 2nd order differential equation of Helmholtz' type:

$$\frac{\partial^2 \varphi(z)}{\partial z^2} - \frac{\varphi(z)}{\delta_\omega^2} = -\frac{q(z)}{\zeta_\omega} \quad (5)$$

where:

| | |
|---|---|
| $\delta_\omega = \frac{\delta}{\sqrt{1 - \omega^2 \tau_a \tau_{tr} + i\omega(\tau_a + \tau_{tr})}}$ | penetration depth for time-harmonic modulation, $[\delta_\omega] = m$ |
| $\delta = \frac{1}{\sqrt{3\mu_{tr}\mu_a}}$ | steady-state penetration depth, $[\delta] = m$ |
| $\zeta_\omega = \frac{\zeta}{1 + i\omega\tau_{tr}}$ | diffusion constant for time-harmonic modulation, $[\zeta_\omega] = m$ |
| $\zeta = \frac{1}{3\mu_{tr}}$ | steady-state diffusion constant, $[\zeta] = m$ |
| $\tau_a = \frac{1}{c\mu_a}$ | absorption relaxation time, $[\tau_a] = m$ |
| $\tau_{tr} = \frac{1}{c\mu_{tr}}$ | transport relaxation time, $[\tau_{tr}] = m$ |

2.2. Layer model

The structures under investigation here consist of two plane layers, the lower one being infinitely extended, the upper one of finite thickness d and bounded by air at its upper surface. The boundaries are assumed to be homogeneously smooth planes, see Fig. 1. Both layers share the same index of refraction n .

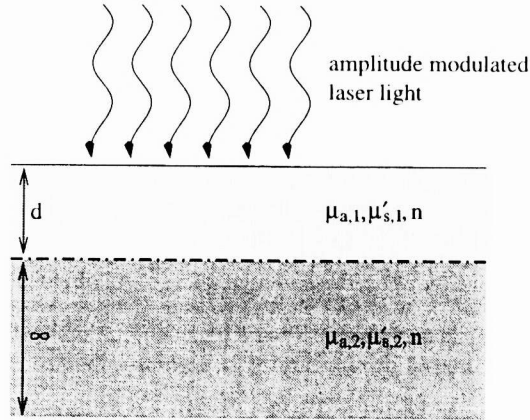


Figure 1. Layer model

If the surface is homogeneously irradiated by perpendicularly incident plane waves of light, a viable description of the source function, i.e. how the light enters the diffusion process, is given by an exponential distribution of isotropic sources in the media:^{20,21}

$$\begin{aligned} q_1(z) &= P_0 \mu'_{s,1} e^{-(\mu_{r,1} + i\omega/c)z} \\ q_2(z) &= P_0 \mu'_{s,2} e^{-(\mu_{r,1} + i\omega/c)d} e^{-(\mu_{r,2} + i\omega/c)(z-d)} \end{aligned} \quad (6)$$

The indices 1 and 2 denote the upper and lower layer, respectively. The imaginary terms account for the phase shift which the modulated light undergoes between the point of entrance at the surface and the point where it is sourced into the diffusion process.

In the given geometry of the structure and with the source function (6), the solution to the differential equation (5) reads as:

$$\begin{aligned}\varphi_1(z) &= \frac{P_0 \delta_{\omega,1}^2 \mu'_{s,1}}{\zeta_{\omega,1} [1 - (\mu_{tr,1} + i\omega/c)^2 \delta_{\omega,1}^2]} e^{-(\mu_{tr,1} + i\omega/c)z} + A_1 e^{-z/\delta_{\omega,1}} + A_2 e^{z/\delta_{\omega,1}} \\ \varphi_2(z) &= \frac{P_0 \delta_{\omega,2}^2 \mu'_{s,2}}{\zeta_{\omega,2} [1 - (\mu_{tr,2} + i\omega/c)^2 \delta_{\omega,2}^2]} e^{-(\mu_{tr,1} + i\omega/c)d} e^{-(\mu_{tr,2} + i\omega/c)(z-d)} + A_3 e^{-z/\delta_{\omega,2}} + A_4 e^{z/\delta_{\omega,2}}\end{aligned}\quad (7)$$

The unknowns $A_1 \dots A_4$ are to be found by application of the boundary conditions. The condition:

$$\lim_{z \rightarrow \infty} \varphi(z) = 0 \quad (8)$$

immediately leads to:

$$A_4 = 0 \quad (9)$$

In between the two layers, both the fluence rate and the flux must be continuous:

$$\varphi_1(z = d^+) = \varphi_2(z = d^-) \quad (10)$$

$$j_1(z = d^+) = j_2(z = d^-) \quad (11)$$

The second condition (11), is to be applied by noticing that for harmonically modulated light (4) writes as:

$$j(z) = -\zeta_{\omega} \frac{d}{dz} \varphi(z) \quad (12)$$

At the outer boundary of the structure, the partial-current boundary condition proposed by Haskell et al.¹⁹ is used:

$$R_{eff} \left(\frac{\varphi_1}{4} - \frac{j_1}{2} \right) \Big|_{z \rightarrow 0^+} = \frac{\varphi_1}{4} + \frac{j_1}{2} \Big|_{z \rightarrow 0^+} \quad (13)$$

The constant R_{eff} , termed the *effective reflection coefficient*, can be found by integrating the Fresnel reflection coefficient over the hemisphere. For boundaries between tissue and air Haskell calculated $R_{eff} = 0.431$ for a refractive index of $n_{tissue} = 1.33$, and $R_{eff} = 0.493$ for $n_{tissue} = 1.4$.

A linear equation system can now be set up from (10), (11) and (13) and solved for the unknowns A_1 , A_2 and A_3 . The fluence rate φ just below the surface is then found from (7), and the flux j at the surface can be determined from (12). The complex diffuse reflection coefficient is defined as:

$$\gamma := -\frac{j|_{z \rightarrow 0^+}}{P_0} \quad (14)$$

and its phase given by:

$$\phi = \arctan \frac{\Im\{\gamma\}}{\Re\{\gamma\}} \quad (15)$$

3. EXPERIMENTAL

In order to investigate the diffuse reflection properties of stratified structures experimentally, 2-layer phantoms were made, with intralipid as the scattering medium. On the bottom of a beaker, a solid layer was formed by fixing intralipid in agar gel. A top layer with varying thickness was then easily obtained by pouring solutions of intralipid on top of the agar layer.

The sample was irradiated by a RF-modulated 674 nm semiconductor laser. From the laser, the light was guided by a 100 μm -core graded index fiber, collimated by a lens attached to the tip of the fiber and subsequently slightly widened again by a microscope lens, such that a circle of about 5 cm diameter was irradiated on the surface of the sample when the microscope lens was kept at a distance of about 20 cm. See Fig. 2 for a sketch of the setup. Thus, it was assured that an area sufficient for measurement was approximately homogeneously irradiated, and that the wavefronts reaching the surface in this area could be considered plane. The reflected light was picked up by a large

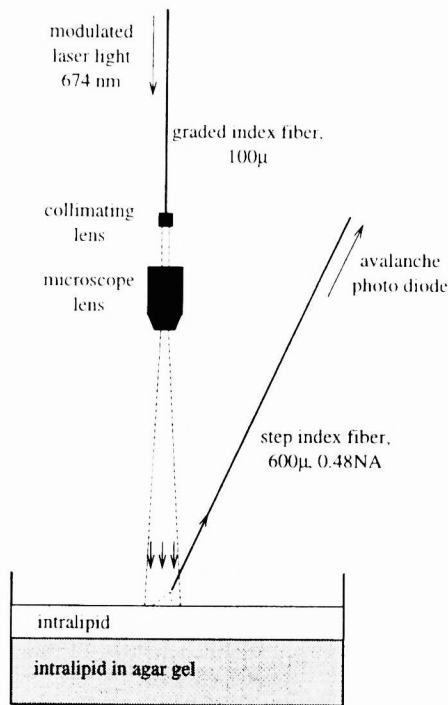


Figure 2. Experimental setup

core step index fiber (600 μm , 0.48 NA). This detector fiber was kept at an angle of about 25° relative to the source fiber in order to avoid specularly reflected light. The distance between the tip of this fiber and the surface was roughly 10 mm. The light picked up from the surface of the phantom was detected by an avalanche photo-diode with lower and upper 3dB roll-off frequencies of 1 MHz and 1 GHz, respectively. A network analyzer (HP8753C) both generated the RF-modulation signal for the laser and analyzed the return signal from the avalanche diode for its phase shift relative to the source signal.

The lowest possible frequency of the signal generator of the network analyzer was 0.3 MHz. At this frequency, the avalanche diode was found to perform well. At the high frequency end, the performance of the avalanche diode deteriorated drastically above 1.5 GHz. As this study aimed at a qualitative investigation of photon-density waves over a wide frequency range, 2 GHz was chosen as the upper modulation frequency limit in order to gain a maximum of information.

In the experiments, a structure with a highly scattering bottom layer and relatively low scattering top layer was investigated. To this end, an agar gel containing 1% of intralipid was made to form the bottom layer. The first measurement was done with a solution of 0.2% intralipid as the top layer. Since the network analyzer summed the phase shift culminating over one sweep over the whole frequency range, the originally recorded values included the frequency response of the whole measurement setup. To eliminate the influence of the system, the phase shift is given here relative to the phase of the reflection coefficient for a zero thickness upper layer, for every given frequency. From the measurement results in Fig. 3 it can be seen that, as the thickness of the upper layer starts to grow, the phase shift increases strongly. For modulation frequencies above 700 MHz, a maximum is formed for an upper layer thickness slightly below 5 mm. Thereafter the phase shift drops off rapidly. At smaller frequencies, the change in phase shift is much stronger at lower than at larger thicknesses, but no distinct maximum can be observed.

In order to investigate the validity of the model, the optical properties were determined from the values given for intralipid by van Staveren and coworkers.²² For adjustment to different concentrations of intralipid, water absorption was added as given by Hale and Query.²³ For the bottom layer, a reduced scattering coefficient of $\mu'_s = 1911 \text{ m}^{-1}$ and an absorption coefficient of $\mu_a = 1.9 \text{ m}^{-1}$ were calculated. The corresponding values for the top layer were $\mu'_s = 238 \text{ m}^{-1}$ and $\mu_a = 0.7 \text{ m}^{-1}$. The influence of agar was neglected at this stage, as its scattering coefficient is

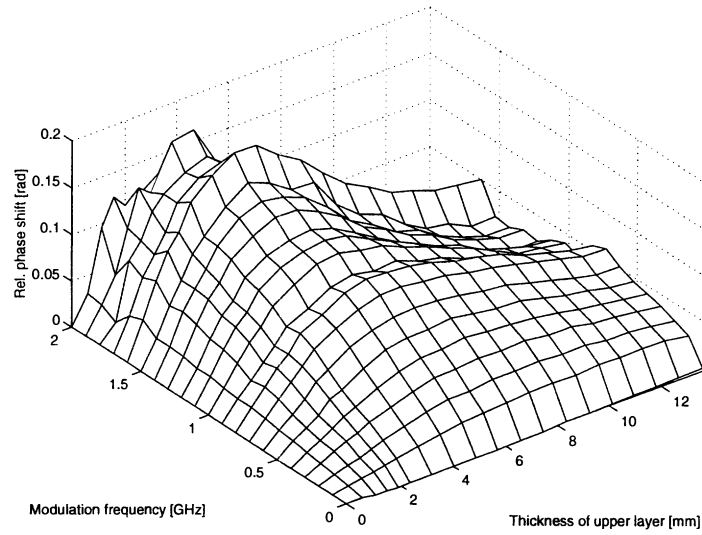


Figure 3. Measured relative phase shift: Bottom layer: 1% intralipid in agar gel; top layer: 0.2% intralipid

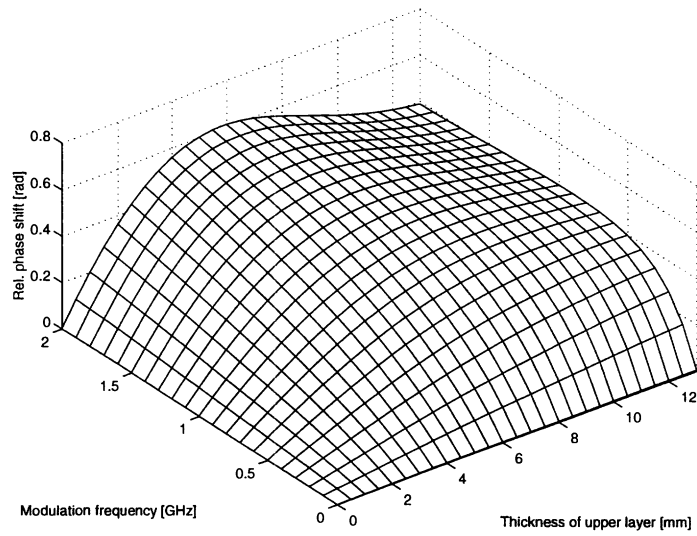


Figure 4. Simulation to Fig.3: Bottom layer: $\mu'_s = 1911 m^{-1}$, $\mu_a = 1.9 m^{-1}$; top layer: $\mu'_s = 238 m^{-1}$, $\mu_a = 0.7 m^{-1}$

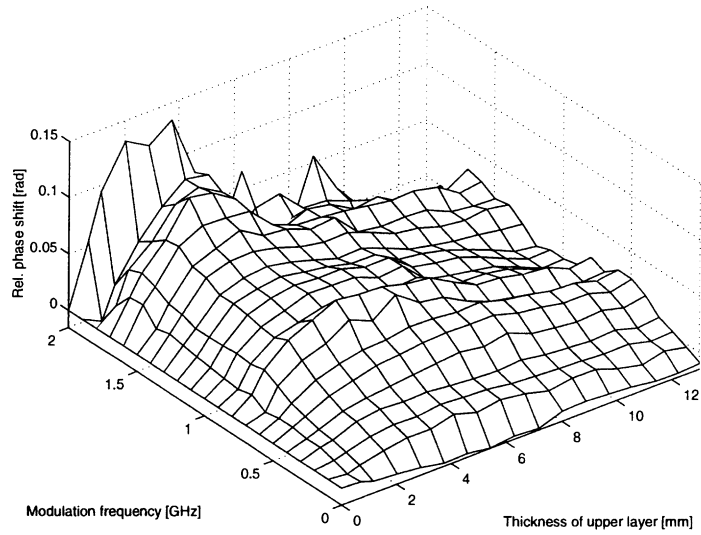


Figure 5. Measured relative phase shift: Bottom layer: 1% intralipid in agar gel; top layer: 0.4% intralipid

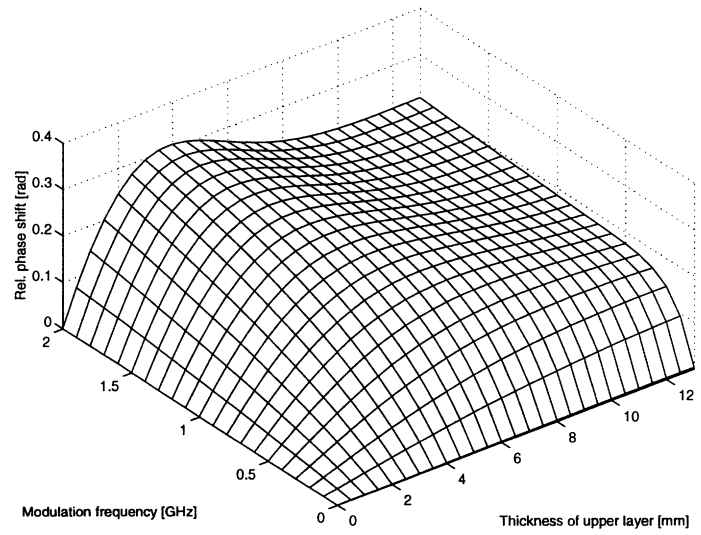


Figure 6. Simulation to Fig.5: Bottom layer: $\mu'_s = 1911 \text{ m}^{-1}$, $\mu_a = 1.9 \text{ m}^{-1}$; top layer: $\mu'_s = 476 \text{ m}^{-1}$, $\mu_a = 1 \text{ m}^{-1}$

negligible in the presence of higher concentrations of intralipid, and experiences with the simulation model showed that small variations in absorption did not lead to significant qualitative changes. The result of the simulation is given in Fig. 4, again normalized to zero for a zero thickness upper layer. In fact, the maximum in phase shift is reestablished, at a thickness of the upper layer of approximately 5 mm. Again, the maximum appears for modulation frequencies higher than 700 MHz. It must be noted, though, that the model does not yet allow for a quantitative analyses, as the simulated phase shift is calculated too high when compared to the measured values.

In order to study the influence of relative changes in the scattering coefficient on the phase shift, a higher intralipid concentration of 0.4% for the top layer was used in the second experiment; the bottom layer was left unchanged. The optical properties of the new upper layer were $\mu'_s = 476 \text{ m}^{-1}$ and $\mu_a = 1 \text{ m}^{-1}$. The measurement results are given in Fig. 5, and Fig. 6 shows the corresponding simulation data. Again a maximum forms for frequencies above 700 MHz, but this time at a smaller thickness of the top layer than before, slightly below 4 mm. Qualitatively the model predicts the correct behavior, quantitatively the problem with exaggerated values in the simulation shows up again. On the other hand, the fact that the maximum of the phase shift reaches only about half the value of the first experiment is correctly reflected in the simulation results.

4. DISCUSSION AND CONCLUSIONS

The phase response of the diffuse reflection coefficient of layered media shows pronounced maxima and minima as the thickness of the top layer and the modulation frequency are varied. This phenomenon must be attributed to the interference of the partial waves propagating in the layers of different optical properties, together with the internal reflection at the boundary of the upper medium to air. Thus, the findings described here might form the base for a technique to analyze the structural properties of stratified tissues non-invasively. A possible application may be found in the determination of the depth of burns.

The two experiments presented in the last section concentrated on the investigation of structures of layers with mainly different scattering properties. It could be shown, both in experiment and simulation, that the position, as well as the amplitude of the phase shift, depend on the scattering coefficients of the two layers. The diffusion model used in this study predicted the behavior of the phase shift phenomenologically correct, but showed weaknesses in quantitative terms. The reason might in parts lie in the source function (6), which is known to underestimate absorption and enforces a phase at all depths that might be incorrect. Nevertheless, the relative difference in phase shift between the first and second experiment was calculated approximately correctly.

The diffusion approximation to the transport equation has shown to be adequate to describe the experimentally observed phenomena. This also means that the boundary conditions, in particular the extended boundary condition applied at the surface to describe internal reflection, are adequate for the description of diffuse-photon density wave propagation.

REFERENCES

1. J. A. Izatt, M. R. Hee, G. M. Owen, E. A. Swanson, and J. G. Fujimoto, "Optical coherence microscopy in scattering media," *Opt. Lett.* **19**, pp. 590–592, April 1994.
2. J. M. Schmitt and A. Knüttel, "Model of optical coherence tomography of heterogenous tissue," *J. Opt. Soc. Am. A* **14**, pp. 1231–1242, June 1997.
3. S. Takatani and M. D. Graham, "Theoretical analysis of diffuse reflectance from a two-layer tissue model," *IEEE Trans. Biomed. Eng.* **26**, pp. 656–664, Dec. 1979.
4. M. Keijzer, W. M. Star, and P. R. M. Storchi, "Optical diffusion in layered media," *Appl. Opt.* **27**, pp. 1820–1824, May 1988.
5. R. Nossal, J. Kiefer, G. H. Weiss, R. Bonner, H. Taitelbaum, and S. Havlin, "Photon migration in layered media," *Appl. Opt.* **27**, pp. 3382–3391, Aug. 1988.
6. H. Taitelbaum, S. Havlin, and G. H. Weiss, "Approximate theory of photon migration in a two-layer medium," *Appl. Opt.* **28**, pp. 2245–2249, June 1989.
7. J. M. Schmitt, G. X. Zhou, and E. C. Walker, "Multilayer model of photon diffusion in skin," *J. Opt. Soc. Am. A* **7**(11), pp. 2141–2153, 1990.
8. W. Cui and L. E. Ostrander, "The relationship of surface reflectance measurements to optical properties of layered biological media," *IEEE Trans. Biomed. Eng.* **39**, pp. 194–201, Feb. 1992.

9. T. J. Farrell, M. S. Patterson, and M. Essenpreis, "Influence of layered tissue architecture on estimates of tissue optical properties obtained from spatially resolved diffuse reflectometry," *Appl. Opt.* **37**, pp. 1958–1972, April 1998.
10. A. Kienle, M. S. Patterson, N. Dögnitz, R. Bays, G. Wagnières, and H. van den Bergh, "Noninvasive determination of the optical properties of two-layered turbid media," *Appl. Opt.* **37**, pp. 779–791, Feb. 1998.
11. L. O. Svaasand, J. Fishkin, B. J. Tromberg, J. You, and M. W. Berns, "Reflectance tomography of layered media with photon density waves," in *International Optical Design Conference*, pp. 153–155, OSA, (Hawaii), June 1998.
12. H. Heusmann, J. Kölzer, and G. Mitic, "Characterization of female breasts *in vivo* by time resolved and spectroscopic measurements in near infrared spectroscopy," *J. Biomed. Opt.* **1**, pp. 425–434, Oct. 1996.
13. J. B. Fishkin, O. Coquoz, E. R. Anderson, M. Brenner, and B. J. Tromberg, "Frequency-domain photon migration measurements of normal and malignant tissue optical properties in a human subject," *Appl. Opt.* **36**, pp. 10–20, Jan. 1997.
14. B. J. Tromberg, L. O. Svaasand, T.-T. Tsay, R. C. Haskell, and M. W. Berns, "Optical property measurements in turbid media using frequency domain photon migration," in *Future Trends in Biomedical Applications of Lasers*, pp. 52–58, SPIE, 1991.
15. L. O. Svaasand, B. J. Tromberg, R. C. Haskell, T.-T. Tsay, and M. W. Berns, "Tissue characterization and imaging using photon density waves," *Optical Engineering* **32**, pp. 258–266, Feb. 1993.
16. J. B. Fishkin and E. Gratton, "Propagation of photon-density waves in strongly scattering media containing an absorbing semi-infinite plane bounded by a straight edge," *J. Opt. Soc. Am. A* **10**, pp. 127–140, Jan. 1993.
17. D. A. Boas, *Diffuse Photon Probes of Structural and Dynamical Properties of Turbid Media: Theory and Biomedical Applications*. PhD thesis, University of Pennsylvania, 1996. <http://dpdw.eotc.tufts.edu/boas/Publications/Dissertation/diss.html>.
18. A. Ishimaru, *Wave Propagation and Scattering in Random Media*, Academic Press, 1978.
19. R. C. Haskell, L. O. Svaasand, T.-T. Tsay, T.-C. Feng, M. S. McAdams, and B. J. Tromberg, "Boundary conditions for the diffusion equation in radiative transfer," *J. Opt. Soc. Am. A* **11**, pp. 2727–2741, Oct. 1994.
20. L. O. Svaasand, L. T. Norvang, E. J. Fiskerstrand, E. K. S. Stopps, M. W. Berns, and J. S. Nelson, "Tissue parameters determining the visual appearance of normal skin and port-wine stains," *Lasers in Medical Science* **10**, pp. 55–65, 1995.
21. T. Spott, L. O. Svaasand, R. E. Anderson, and P. F. Schmedling, "Application of optical diffusion theory to transcutaneous bilirubinometry," in *Laser-Tissue Interaction, Tissue Optics, and Laser Welding III*, vol. 3195 of *SPIE Proceedings*, pp. 234–245, SPIE, (San Remo), Sep. 1997.
22. H. J. van Staveren, C. J. M. Moes, J. van Marchle, S. A. Prahl, and M. J. C. van Gemert, "Light scattering in intralipid-10% in the wavelength range of 400–1100nm," *Appl. Opt.* **30**, pp. 4507–4514, Nov. 1991.
23. G. M. Hale and M. R. Querry, "Optical constants of water in the 200-nm to 200- μ m wavelength region," *Appl. Opt.* **12**, pp. 555–563, March 1973.